



CHORUS

This is the accepted manuscript made available via CHORUS. The article has been published as:

## Scaling and Statistics in Three-Dimensional Compressible Turbulence

Jianchun Wang, Yipeng Shi, Lian-Ping Wang, Zuoli Xiao, X. T. He, and Shiyi Chen

Phys. Rev. Lett. **108**, 214505 — Published 25 May 2012

DOI: [10.1103/PhysRevLett.108.214505](https://doi.org/10.1103/PhysRevLett.108.214505)

# Scaling and statistics in three-dimensional compressible turbulence

J. Wang<sup>1</sup>, Y. Shi<sup>1</sup>, L.-P. Wang<sup>2</sup>, Z. Xiao<sup>1</sup>, X. T. He<sup>1</sup>, and S. Chen<sup>1\*</sup>

<sup>1</sup> *SKLTCS and CAPT, College of Engineering,  
Peking University, Beijing 100871, China*

<sup>2</sup> *Department of Mechanical Engineering,  
University of Delaware, Newark, DE19716, USA*

(Dated: March 19, 2012)

The scaling and statistical properties of three-dimensional (3D) compressible turbulence are studied using high-resolution numerical simulations and a heuristic model. The two-point statistics of solenoidal component of the velocity field are found to be no significantly different from those of incompressible turbulence, while the scaling exponents of the velocity structure function for the compressive component become saturated at high orders. Both the simulated flow and the heuristic model reveal the presence of a power-law tail in the probability density function (PDF) of negative velocity divergence (high compression regime). The power-law exponent is different from that in Burgers turbulence, and this difference is shown to have a major contribution from the pressure effect which is absent in the Burgers turbulence.

PACS numbers: 47.27.E-, 47.40.ki, 47.53.+n

Compressible three-dimensional (3D) fluid turbulence is of great importance to a large number of industrial applications and natural phenomena, including high-temperature reactive flows, transonic and hypersonic aircrafts, inter-planet space exploration, and star-forming clouds in galaxies [1]. An accurate description (e.g., SGS modeling [2]) of small-scale compressible turbulence is desired when modeling complex compressible turbulence. In this paper, we study the effects of compressibility and shock discontinuities on the statistics of fluid turbulence, with a specific attention on the similarity and difference between 3D compressible turbulence and one-dimensional Burgers turbulence.

Since it is difficult to analyze 3D compressible turbulence, Burgers [3] first systematically studied a nonlinear model of fluid turbulence, i.e., the one-dimensional Burgers equation. Since then, the one-dimensional Burgers turbulence has frequently been investigated theoretically and numerically [4–13]. According to multifractal theory [4], isolated shocks connected by smooth ramps lead to bifractal scaling exponents of velocity structure function in the Burgers turbulence. Mitra et al. [5] performed simulation of one-dimensional Burgers turbulence with up to  $2^{20}$  mesh points to study multiscaling of velocity structure functions. They found that scaling exponents asymptotically saturates to one with increasing orders. Much effort has also been made to exploit the asymptotic behavior at the tail of PDF of negative velocity derivative in Burgers turbulence [7–13]. E et al. [10] predicted that the large negative velocity gradients stem mainly from preshocks, leading to the  $-7/2$  power-law tail in the PDF of negative velocity gradients (provided that preshocks do not cluster). Bec [11] verified this result using a novel particle and shock tracking numerical method. Boldyrev et al. [12] carried out simulations of random forced Burgers turbulence using a standard shock capturing scheme.

They obtained a power-law exponent of about  $-3.4$ , very close to the theoretical value of  $-3.5$ .

Compared to incompressible turbulence, 3D compressible turbulence is more complex due to nonlinear interactions between solenoidal and compressive modes of velocity fluctuations, and furthermore couplings between velocity field and pressure field [14]. Besides the vortex-filament induced intermittency observed in the incompressible turbulence, shock waves in the compressible turbulence add an intermittent dissipation mechanism of different topological structures [15]. Schmidt et al. [16] studied two-point velocity statistics of compressible turbulence at rms Mach number of 5.5 by numerical simulations of Euler equations. A universal scaling has been recovered by reformulation of the refined similarity hypothesis in terms of the mass-weighted velocity  $\rho^{1/3}\mathbf{u}$ . They also reported that the most intermittent dissipative structures were shocks, due to extreme compressibility of the flow field. Galtier and Banerjee [17] derived an exact relation for correlation functions in compressible isothermal turbulence that mimics the Kolmogorov 4/5 law in the incompressible isotropic turbulence. Consequently, they theoretically revealed the effect of dilation and compression on the local energy transfer. By dimensional arguments, they further obtained a  $k^{-5/3}$  spectrum of density-weighted velocity  $\rho^{1/3}\mathbf{u}$ .

Here a forced compressible turbulence is simulated in a cubic box with periodic conditions at  $1024^3$  grid-resolution, using a novel hybrid approach described in [18] (also see Supplementary Material). A total of 20 flow fields at the statistical stationary stage spanning  $2.68 \leq t/T_e \leq 4.63$  are extracted to analyze the flow statistics, where  $t$  is time and  $T_e$  is the large eddy turnover time defined by  $T_e = \sqrt{3}L/u'$ , where  $L$  is the integral length scale and  $u'$  is the root-mean-square (r.m.s.) velocity magnitude. The turbulent Mach number is

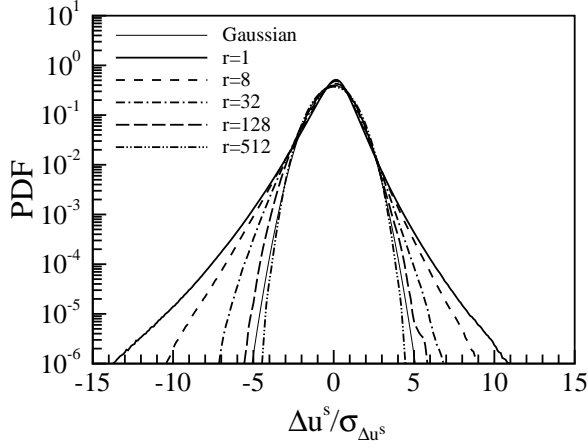


FIG. 1: Normalized probability density functions of  $\Delta u^s$ .

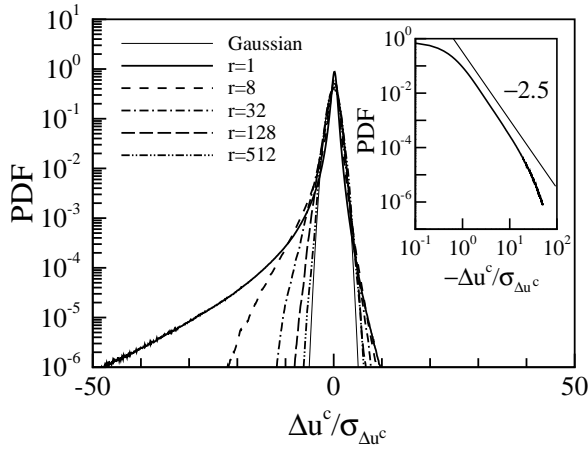


FIG. 2: Normalized probability density functions of  $\Delta u^c$ . **Inset:** log-log plot of the same PDF for the negative  $\Delta u^c$  at the one-grid-length separation.

$M_t = u'/\langle c \rangle = 1.03$  and Taylor microscale Reynolds number is  $R_\lambda = 254$ , where  $\langle c \rangle$  is the average sound speed. The r.m.s. velocity divergence is found to be  $\theta' = 0.35\omega'$ , where  $\omega'$  is the r.m.s. vorticity magnitude. **It is also found (not shown in the paper) that power spectra for velocity  $\mathbf{u}$ , density-weighted velocity  $\rho^{1/3}\mathbf{u}$  and  $\rho^{1/2}\mathbf{u}$  almost overlap, indicating a minor effect of density fluctuations on the velocity spectrum.**

In order to reveal the underlying physics in the compressible turbulence, we employ the Helmholtz decomposition [14], namely, the fluid velocity  $\mathbf{u}$  is decomposed into a solenoidal component  $\mathbf{u}^s$  and a compressive component  $\mathbf{u}^c$ :  $\mathbf{u} = \mathbf{u}^s + \mathbf{u}^c$ , where  $\nabla \cdot \mathbf{u}^s = 0$  and  $\nabla \times \mathbf{u}^c = 0$ . In our simulated flow, the ratio of r.m.s. fluctuations,  $u^c/u^s$ , is found to be 0.22, comparable to 0.18 reported in Porter et al. [19] at a similar turbulent Mach number.

Fig. 1 shows the normalized PDFs of the longitudinal increments,  $\Delta u^s(r) \equiv \Delta \mathbf{u}^s(\mathbf{r}) \cdot \mathbf{r}/r$ , of the solenoidal velocity component at different separations, where  $\mathbf{r}$  is

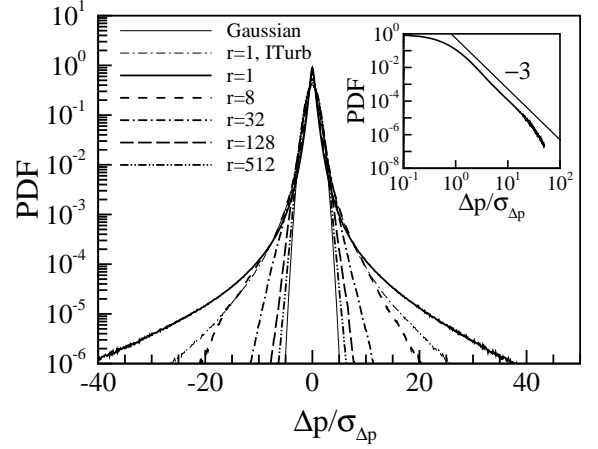


FIG. 3: Normalized probability density functions of  $\Delta p$ . **Thin dash-dotted line is the corresponding PDF at the one-grid-length separation for incompressible turbulence (ITurb) at the same Taylor Reynolds number. Inset:** log-log plot of the PDF for positive  $\Delta p$  in compressible turbulence at the one-grid-length separation.

the separation vector and  $r = |\mathbf{r}|$ . The PDFs exhibit **stretched exponential tails** at small spatial separations and approach to Gaussian as the separation increases. These trends are very similar to those found in incompressible turbulence [20]. Fig. 2 shows the normalized PDFs of the longitudinal increments,  $\Delta u^c(r) \equiv \Delta \mathbf{u}^c(\mathbf{r}) \cdot \mathbf{r}/r$ , of the compressive velocity component. The shape of PDFs is highly skewed at small separations and always has longer tail than Gaussian for all separations. In addition, at the one-grid-length separation, the PDF has a power-law tail with an exponent of  $-2.5$  on the left side. **We note that due to the power law behavior of the PDF tail, when the viscosity asymptotically approaches zero, special care is required since the variance of velocity increment may become unbounded.** Similar results have been reported for the Burgers turbulence. In the random-force driven Burgers turbulence, the PDFs of velocity increments have an algebraic tail at left side, leading to strong intermittency and bifractality of scaling exponents [8].

We plot the normalized PDFs of the pressure increments  $\Delta p$  in Fig. 3. The shapes of these PDFs are nearly symmetric and have longer tails at small spatial separations than those in the incompressible turbulence **at the same Taylor Reynolds number (also see [21])**. The pressure changes drastically in the high compression regime, leading to intensive pressure increments at small separations. Power-law tails are also found in the pressure-increment PDF at the one-grid-length separation, with an power-law exponent of  $-3$ .

The scaling exponents for the longitudinal structure

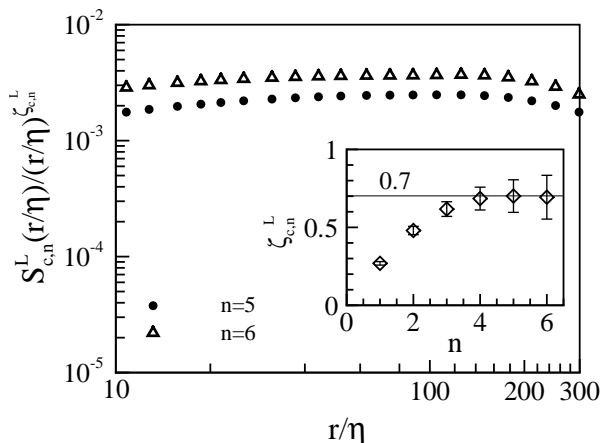


FIG. 4: Compensated structure functions for  $n = 5, 6$ , as a function of normalized separation. Inset: scaling exponents  $\zeta_{c,n}^L$  as a function of  $n$ . The separation  $r$  is normalized by Kolmogorov length scale  $\eta = [\langle \nu \rangle^3 / \epsilon]^{1/4}$ , where  $\nu$  is the kinematic viscosity and  $\epsilon$  is the kinetic energy dissipation rate.

functions in the inertial subrange are defined as

$$S_{s,n}^L(r) \equiv \left\langle \left| \Delta u^s(r) \right|^n \right\rangle \sim r^{\zeta_{s,n}^L}, \quad (1)$$

$$S_{c,n}^L(r) \equiv \left\langle \left| \Delta u^c(r) \right|^n \right\rangle \sim r^{\zeta_{c,n}^L}, \quad (2)$$

where  $\zeta_{s,n}^L$  and  $\zeta_{c,n}^L$  are the scaling exponents for the two velocity components, respectively. Our results show that  $\zeta_{s,n}^L$  agrees well with those from the incompressible turbulence [22, 23]. This implies that at  $M_t \sim 1$ , the two-point statistics of solenoidal velocity component are insensitive to the presence of shocks. **In addition, similar to results in [19, 24], we find that the scaling exponents of the full velocity  $\mathbf{u}$  are also the same as those in the incompressible turbulence.** However, the scaling exponents of the the compressive velocity component, shown in the insert of Fig. 4, is drastically different. A saturation of  $\zeta_{c,n}^L$  is observed for  $n \geq 5$ , and the saturated value is estimated to be  $\zeta_{c,\infty}^L \approx 0.7$ . The compensated longitudinal structure functions at orders 5 and 6 are shown in Fig. 4, where the separation is normalized by Kolmogorov length  $\eta$ . **According to the multi-fractal theory, the saturation of exponents is caused by the domination of frontlike structures [24]. Benzi et al. [24] observed that density field displays frontlike structures, leading to saturation of scaling exponents for density structure functions in a weakly compressible turbulence at rms Mach number 0.3. However, for the velocity field, they did not find any difference between weakly compressible turbulence and incompressible turbulence. On the other hand, due to relatively higher turbulent Mach number in our simulated flow, shocks produce a significant number of front-like structures in the compressive velocity field, causing saturation of scaling exponents  $\zeta_{c,n}^L$ . Furthermore, substantial uncertainties in the exponents at high orders are**

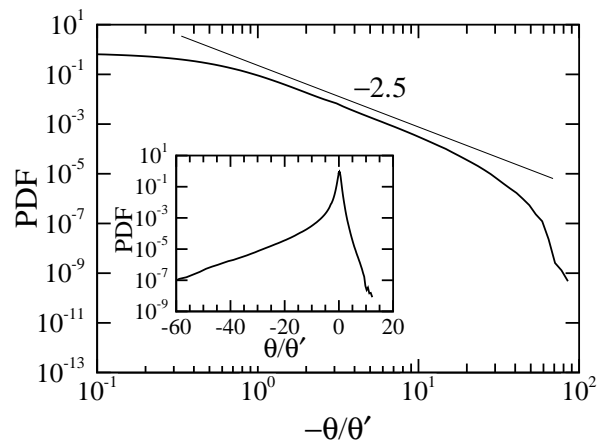


FIG. 5: Probability density function of velocity divergence.

**associated with large temporal fluctuations, which ascribe to instability of intermittency structures [25].**

The PDF of velocity divergence (Fig. 5) exhibits a power-law tail for large negative divergence and an super-exponential tail for large positive divergence, both qualitatively similar to the PDF of velocity derivative in Burgers turbulence [13]. In Burgers turbulence with infinitesimal viscosity, the large negative velocity gradients stem mainly from preshocks, leading to the power-law tail in the PDF of negative velocity gradients [10]. In the compressible turbulence, through studying the contours of velocity divergence (not shown here), we have identified that the power-law regime of velocity divergence have a major contribution from preshocks and weak shocklets rather than strong shock waves. Otherwise, the power-law exponent for the PDF of velocity divergence is  $-2.5$ , the same as that for the PDF of the longitudinal increments of compressive velocity component at the one-grid-length separation, but qualitatively different from the power-law exponent ( $-3.5$ ) for the PDF of velocity gradient in one-dimensional Burgers turbulence. To understand this difference, we write down the equation of the velocity derivative in Burgers turbulence [9]

$$\frac{\partial \xi}{\partial t} + u \frac{\partial \xi}{\partial x} = -\xi^2 + \nu \frac{\partial^2 \xi}{\partial x^2} + \frac{\partial f}{\partial x}, \quad (3)$$

where  $u(x, t)$  is velocity and  $\xi(x, t)$  is velocity gradient. The forcing  $f(x, t)$  is used to maintain the Burgers turbulence to be statistically stationary. In contrast, the governing equation for velocity divergence in 3D Navier-Stokes flow is:

$$\frac{\partial \theta}{\partial t} + u_j \frac{\partial \theta}{\partial x_j} = -\frac{\partial u_j}{\partial x_i} \frac{\partial u_i}{\partial x_j} - \frac{1}{\gamma M^2} \frac{\partial}{\partial x_i} \left( \frac{1}{\rho} \frac{\partial p}{\partial x_i} \right) + \frac{4\nu_0}{3Re} \frac{\partial^2 \theta}{\partial x_i^2}. \quad (4)$$

To simplify the discussions, we have neglected the effect of density fluctuations on the viscous term. It is seen that there are some similarities between the term  $\frac{\partial u_j}{\partial x_i} \frac{\partial u_i}{\partial x_j}$

in Eq. (4) and  $\xi^2$  in Eq. (3), the former causing strong skewness of PDF for velocity divergence provided turbulent Mach number is larger than 0.3 [26].

Below, we demonstrate how the pressure term alters the power-law exponent of the PDF of velocity divergence in high compression regime. Following the similar procedure provided by Gotoh and Kraichnan [6], we can derive the Liouville equation for the PDF of velocity divergence  $P(\theta)$  as follows (see Supplementary Material):

$$\frac{\partial P}{\partial t} - \frac{\partial(\theta^2 P)}{\partial \theta} - \theta P + D = F, \quad (5)$$

where the dissipation term is

$$D(\theta) = \frac{4\nu_0}{3Re} \frac{\partial}{\partial \theta} \left[ \left\langle \frac{\partial^2 \theta}{\partial x_i^2} \middle| \theta \right\rangle P \right] \quad (6)$$

and the *forcing* term including effects of pressure and anisotropic straining is

$$F = \frac{\partial}{\partial \theta} \left[ \left\langle \frac{1}{\gamma M^2} \frac{\partial}{\partial x_i} \left( \frac{1}{\rho} \frac{\partial p}{\partial x_i} \right) + \left( \frac{\partial u_j}{\partial x_i} \frac{\partial u_i}{\partial x_j} - \theta^2 \right) \middle| \theta \right\rangle P \right]. \quad (7)$$

This equation is written formally the same as the PDF equation of velocity derivative in Burgers turbulence, but with different **dissipation term and forcing term** [13]. It has been argued previously [7–13] that Burgers turbulence has a power-law tail in the PDF of  $\xi$  for high compression regime. If Burgers turbulence is driven by large scale white-in-time random forcing, this tail is believed to be universal with an exponent  $-3.5$  in the limit of vanishing viscosity. Other exponents are possible if Burger turbulence is driven by forcing with prescribed power-law spectra [8].

In Fig. 6, we plot the average normalized straining  $\frac{1}{\theta^2} \frac{\partial u_j}{\partial x_i} \frac{\partial u_i}{\partial x_j}$  conditioned on the velocity divergence, as a function of velocity divergence. For the compression regime (*i.e.*,  $\theta < 0$ ), we find that the straining term can be well approximated by  $\frac{\theta^2}{\theta^2}$ , implying that the effect of stretching-tilting dynamics on the PDF of velocity divergence is small. In addition, its compressive component  $\frac{1}{\theta^2} \frac{\partial u_j^c}{\partial x_i} \frac{\partial u_i^c}{\partial x_j}$  dominates the overall straining term. These interesting approximations are consistent with the numerical simulations that intensive velocity gradients are dominated by variations in one spatial direction during compression in the shock waves [14, 27]. Therefore, the solenoidal velocity component has very limited contribution to the PDF equation of velocity divergence in the compression regime. In contrast, in the expansion regime (*i.e.*,  $\theta > 0$ ), the straining term is no longer close to square of divergence. Based on dimensional analysis, the anisotropic straining term  $(\frac{1}{\theta^2} \frac{\partial u_j}{\partial x_i} \frac{\partial u_i}{\partial x_j} - (\frac{\theta}{\theta'})^2)$  can be represented by square of divergence multiplying by a non-dimensional constant. Fig. 6 shows that this non-dimensional constant is around  $-0.8$  in the expansion regime instead of almost zero in the compression

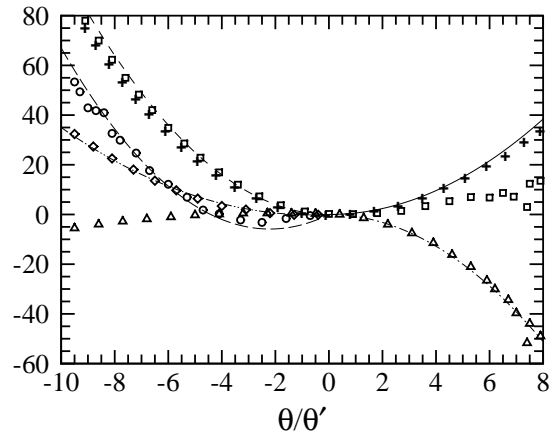


FIG. 6: Conditional average of  $\left\langle \frac{1}{\theta^2} \frac{\partial u_j}{\partial x_i} \frac{\partial u_i}{\partial x_j} \middle| \frac{\theta}{\theta'} \right\rangle$  (squares),  $\left\langle \frac{1}{\theta^2} \frac{\partial u_j^c}{\partial x_i} \frac{\partial u_i^c}{\partial x_j} \middle| \frac{\theta}{\theta'} \right\rangle$  (plus),  $\left\langle \frac{1}{\theta^2} \frac{\partial u_j}{\partial x_i} \frac{\partial u_i}{\partial x_j} - \left( \frac{\theta}{\theta'} \right)^2 \middle| \frac{\theta}{\theta'} \right\rangle$  (triangles),  $\left\langle \frac{1}{\theta^2} \frac{4\nu_0}{3Re} \frac{\partial^2 \theta}{\partial x_i^2} \middle| \frac{\theta}{\theta'} \right\rangle$  (diamonds) and  $\left\langle \frac{1}{\theta^2} \frac{1}{\gamma M^2} \frac{\partial}{\partial x_i} \left( \frac{1}{\rho} \frac{\partial p}{\partial x_i} \right) \middle| \frac{\theta}{\theta'} \right\rangle$  (circles). The lines represent  $\alpha \left( \frac{\theta}{\theta'} \right)^2 + \beta \frac{\theta}{\theta'}$  with  $(\alpha, \beta) = (1.0, 0.0)$  (dashed line),  $(\alpha, \beta) = (0.6, 0.0)$  (solid line),  $(\alpha, \beta) = (-0.8, 0.0)$  (dash-dotted line),  $(\alpha, \beta) = (0.4, 0.5)$  (dash-dot-dotted line) and  $(\alpha, \beta) = (1.2, 5.3)$  (long dashed line).

regime. The conditional straining is always positive, implying that the magnitude of the velocity divergence is increased by the straining when  $\theta < 0$ , but it is decreased by the straining when  $\theta > 0$ . However, the magnitude of the conditional straining for  $\theta > 0$  is only about 1/5 the values for  $\theta < 0$ , indicating that the effect of straining on the velocity divergence is substantially weaker in the expansion regime. Therefore, the role of the straining term in Eq. (4) is similar to that of  $\xi^2$  term in Eq. (3) in the compression regime due to shock structures; but in the expansion regime, it is weakened by relaxation of multi-directional advection and by the solenoidal velocity dynamics, where the flow are dominated by vortex structures.

We now focus our discussion on the PDF equation in the strong compression regime where the power-law tail appears. In Fig. 6, we show average values of viscous term and pressure term conditioned on  $\theta$  in the PDF equation. As also shown in the figure, the anisotropic straining effect is small compared with the other two terms, and may be neglected. The viscous term is well fitted by a parabola  $\alpha_\nu \left( \frac{\theta}{\theta'} \right)^2 + \beta_\nu \frac{\theta}{\theta'}$  with  $\alpha_\nu = 0.4$  and  $\beta_\nu = 0.5$ . A similar procedure was suggested by Gotoh et. al [9] based on an analysis of viscous term inside an equilibrium single-shock in Burgers turbulence. Pressure term can also be approximated by a parabola with coefficient  $\alpha_p = 1.2$  and  $\beta_p = 5.3$ . With these approximations, we obtain the following solution at the stationary stage

$$P(\theta) = C_0 \theta^{-1} \left[ \theta + \frac{(\beta_\nu - \beta_p)}{1 + \alpha_p - \alpha_\nu} \right]^{-1 - \frac{1}{1 + \alpha_p - \alpha_\nu}}. \quad (8)$$

It follows that, for large negative  $\theta$ ,  $P(\theta) \propto \theta^{-q}$  with the exponent being  $q = 2 + \frac{1}{1 + \alpha_p - \alpha_\nu}$ . Using the fitting values for  $\alpha_p$  and  $\alpha_\nu$ , we then obtain  $q = 2.56$ . This is very close to the value of 2.5 shown in Fig. 5. An exponent of  $-3$  is obtained without considering the pressure term and viscous term, which is consistent with the case of Burgers turbulence [13]. The viscous term enlarges the exponent as in Burgers turbulence [13]. The key difference here is the modification of the power-law exponent from the pressure term. We note that the role of the pressure is opposite to that of the viscosity in determining this exponent, and the effect of pressure predominates.

Finally, we emphasize that the viscosity is small but finite in our discussion on the PDF of velocity divergence. Several issues require further investigations, including the relative contributions of preshocks and weak shocklets to the power-law tail of the PDF at higher Reynolds numbers, the asymptotic behavior of the power-law exponent in the limit of vanishing viscosity, and the effect of Mach number on the power-law behavior.

We thank Qionglin Ni, Zhenhua Xia and Zhou Jiang for many useful discussions. This work was supported by the National Natural Science Foundation of China (Grant No.10921202) and the National Science and Technology Ministry under a sub-project of the 973 program (Grant No. 2009CB724101). Simulations were done on a cluster computer in the Center for Computational Science and Engineering at Peking University, China and on Bluefire at NCAR, USA through CISEL-35751014 and CISEL-35751015. L.P.W. acknowledges support from the US National Science Foundation under grants ATM-0730766 and OCI-0904534.

---

\* Electronic address: [syc@pku.edu.cn](mailto:syc@pku.edu.cn)

- [1] P. Padoan and A. Norlund, *Astrophys. J.* **576**, 870 (2002)  
 [2] B. Kosovic, D.I. Pullin, and R. Samtaney, *Phys. Fluids*, **4**, 1511-1522 (2002).  
 [3] J. M. Burgers, *Advances in Applied Mechanics* (Academic, New York, 1948), Vol. I, pp. 171-199.  
 [4] E. Aurell, U. Frisch, J. Lutsko, and M. Vergassola, *J. Fluid. Mech.* **238**, 467 (1992)  
 [5] D. Mitra, J. Bec, R. Pandit, and U. Frisch, *Phys. Rev. Lett.* **94**, 194501 (2005)  
 [6] T. Gotoh and R.H. Kraichnan, *Phys. Fluids A* **5**, 445 (1993).  
 [7] A. M. Polyakov, *Phys. Rev. E* **52**, 6183 (1995)  
 [8] A. Chekhlov and V. Yakhot, *Phys. Rev. E* **52**, 5681 (1995)  
 V. Yakhot and A. Chekhlov, *Phys. Rev. Lett.* **77**, 3118 (1996)  
 [9] T. Gotoh and R.H. Kraichnan, *Phys. Fluids* **10**, 2859 (1998).  
 [10] W. E, K. Khanin, A. Mazel, and Ya. Sinai, *Phys. Rev. Lett.* **78**, 1904 (1997)  
 [11] J. Bec, *Phys. Rev. Lett.* **87**, 104501 (2001)  
 [12] S. Boldyrev, T. Linde, and A. Polyakov, *Phys. Rev. Lett.* **93**, 184503 (2004)  
 [13] J. Bec and K. Khanin, *Phys. Rep.* **447**, 1 (2007)  
 [14] R. Samtaney, D. I. Pullin, and B. Kosovic, *Phys. Fluids* **13**, 1415-1430 (2001).  
 [15] L. Pan, P. Padoan, and A. G. Kritsuk *Phys. Rev. Lett.* **102**, 034501 (2009).  
 [16] W. Schmidt, C. Federrath, and R. Klessen *Phys. Rev. Lett.* **101**, 194505 (2008).  
 [17] S. Galtier, and S. Banerjee *Phys. Rev. Lett.* **107**, 134501 (2011).  
 [18] J. Wang, L.-P. Wang, Z. Xiao, Y. Shi, and S. Chen, *J. Comp. Phys.* **229**, 5257-5279 (2010).  
 [19] D. Porter, A. Pouquet, and P. Woodward, *Phys. Rev. E.* **66**, 026301 (2002).  
 [20] S. Chen, G. D. Doolen, R. H. Kraichnan, and Z. She, *Phys. Fluids A* **5**, 458 (1993).  
 [21] N. Cao, S. Chen, and G. D. Doolen, *Phys. Fluids* **11**, 2235 (1999).  
 [22] Z. S. She and E. L ev eque, *Phys. Rev. Lett.* **72**, 336 (1994).  
 [23] N. Cao, S. Chen, and Z. S. She, *Phys. Rev. Lett.* **76**, 3711 (1996).  
 [24] R. Benzi, L. Biferale, R.T. Fisher, L.P. Kadanoff, D.Q. Lamb, and F. Toschi, *Phys. Rev. Lett.* **100**, 234503 (2008).  
 [25] S. Chen and N. Cao, *Phys. Rev. Lett.* **78**, 3459 (1997).  
 [26] S. Pirozzoli and F. Grasso, *Phys. Fluids* **16**, 4386 (2004).  
 [27] J. Wang, Y. Shi, L.-P. Wang, Z. Xiao, X. He, and S. Chen, *Phys. Fluids* **23**, 125103 (2011).